Two-level Energy Management Strategy for a Fuel Cell-Battery-Ultracapacitor Hybrid System

Chen Zhao, He Yin
Univ. of Michigan-Shanghai Jiao Tong Univ. Joint Institute,
Shanghai Jiao Tong University,
Shanghai, P. R. China
Email: zc437041363@sjtu.edu.cn
yyy@sjtu.edu.cn

Chengbin Ma*[1,2]
1. Univ. of Michigan-Shanghai Jiao Tong Univ. Joint Institute,
2. School of Mechanical Engineering,
Shanghai Jiao Tong University,
Shanghai, P. R. China
Email: chbma@sjtu.edu.cn

***Abstract*—This paper provides a two-level energy management strategy for a fuel cell-battery-ultracapacitor (UC) hybrid system. In the proposed strategy, the battery and UC packs are seen as an energy storage system (ESS) at the first level and the equivalent consumption minimization strategy is used to distribute load power between this ESS and the fuel cell system. The penalty factor is tuned based on estimated average load power and SOC of the ESS. At the second level, the power distribution between the battery and UC packs is determined using the equivalent series resistance-based control strategy to minimize the energy loss. Then, the performance of the proposed two-level energy management strategy is analyzed in simulation under a realistic load profile. Finally, detailed comparison results show that the two-level energy management strategy can achieve lower hydrogen consumption, compared with the rule-based method.**

***Index Terms*—Battery, Energy management strategy, Fuel cell, Hybrid sytem, Ultracapacitor**

I. Introduction

With the rapid increase in greenhouse gas emission, the fuel cell technology can be seen as a good candidate to replace the internal combustion engine (ICE) due to its high efficiency and zero emission [1]. Due to the slow response time of the fuel cell system, fast changing load demand would lead to fuel starvation phenomenon, which will shorten its lifespan [2]. One of common solutions is to use an energy storage system (ESS) as a buffer to isolate the fuel cell system from the dynamic load demand [3]. Therefore, the fuel cell system can be designed to supply the constant average power at its high-efficiency region with low fuel consumption and long lifespan [4].

Batteries and ultracapacitors (UCs) can be seen as two promising energy storage devices in the fuel cell based hybrid system [4]–[6]. Experimental results show that the efficiency and specific power density of the fuel cell-battery hybrid system is higher than that of the fuel cell system alone [7]. Because UCs have higher power density and longer cycle life than batteries, the fuel cell-UC hybrid system shows a lower cost compared to the fuel cell-battery hybrid system [8], [9]. However, due to the limited energy density of UCs, the fuel cell-UC hybrid system may malfunction during the fuel cell start-up time [4]. Therefore, the battery-UC hybrid system is proposed as the ESS to assist the fuel cell system [4], [9], [10]. The comparative studies show that the fuel cell-battery-UC hybrid system has higher fuel economy than fuel cell-battery and fuel cell-UC hybrid systems [5], [6].

In the fuel cell-battery-UC hybrid system, many energy management strategies have been proposed. A set of operation states are defined to determine the output power of each device [11], [12]. Model predictive control is proposed to restrict the current slope of fuel cell and stabilize the dc bus voltage based on its linearized state-space model [13], [14]. A power sharing strategy based on fuzzy logic and wavelet transform is proposed to distribute load demand among different energy devices based on their response times [15]. For a better fuel economy, the equivalent consumption minimization strategy (ECMS) is proposed to minimize the equivalent fuel consumption in the fuel cell based hybrid system [16]. Since it is a realization of the Pontryagin's minimum principle (PMP) for on-line implementation purposes, ECMS with well-tuned parameters guarantees a near-optimal performance [17]. The ECMS is first used in the fuel cell-battery-UC hybrid system to determine the power of the fuel cell system [18]. Since the SOC of UCs is simply controlled to the predefined value, the proposed strategy in [18] does not guarantee an overall optimal performance.

In this paper, a two-level energy management strategy is proposed for the fuel cell-battery-UC hybrid system. In the proposed two-level energy management strategy, the load power is distributed between the fuel cell system and the battery-UC hybrid system using the ECMS to minimize the total hydrogen consumption at the first level. At the second level, the power flow between battery and UC packs is determined using the equivalent series resistance (ESR)-based method. Then, the performance of the two-level energy management strategy is analyzed in simulations. Finally, the proposed energy management strategy is compared with the rule-based strategy in terms of the hydrogen consumption.

II. Fuel cell-Battery-UC Hybrid System

A. Fuel Cell System

In the proposed hybrid system, a 100 W proton exchange membrane fuel cell (PEMFC) system from Heliocentris is used, in which 20 cells with active surface area (A) of 25

cm^2 are connected in series [19]. Its hydrogen mass flow rate $\dot{m}_{H_2,f}$ is approximated as a quadratic function of its output power P_f, which is calculated as

$$\dot{m}_{H_2,f} = a_{f_0} P_f^2 + a_{f_1} P_f + a_{f_2}, \tag{1}$$

where a_{f_0}, a_{f_1}, a_{f_2} are obtained by fitting the original hydrogen consumption model from [19]. Fig. 1(a) shows that the quadratic hydrogen consumption model is accurate enough for fuel cell system, and is used in the following system-level analysis [20]. Then, the efficiency of the fuel cell system η_f is calculated as

$$\eta_f = \frac{P_f}{\dot{m}_{H_2,f} \mathrm{LHV}_{H_2}}, \tag{2}$$

where LHV_{H_2} is the low heat value of the hydrogen. Fig. 1(b) shows that the efficiency of the fuel cell system reaches its maximum value when its output power P_f is 22.6 W.

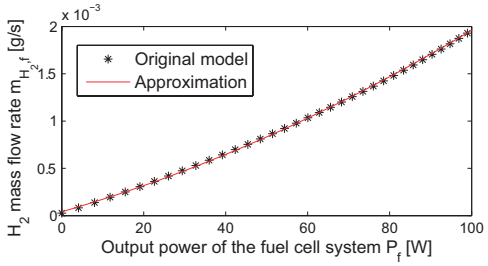

(a)

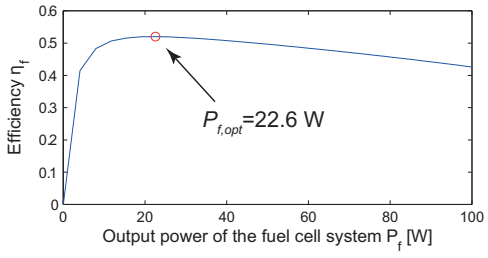

(b)

Fig. 1. Efficiency and hydrogen mass flow rate $\dot{m}_{H_2,f}$ of the fuel cell system. (a) Hydrogen mass flow rate $\dot{m}_{H_2,f}$. (b) Efficiency.

B. Energy Storage System

The ESS combines battery and UC packs using the capacitor semiactive topology, as shown in Fig. 2.

1) Battery: In this system-level analysis, the Rint model is used to calculate the power loss of the lithium-ion battery pack, as shown in Fig. 2. $V_{o,b}$ and $R_{s,b}$ are the open circuit voltage (OCV) and the series resistance of the battery pack, respectively, which are calculated as

$$V_{o,b} = a_0 + a_1 x + a_2 x^2 + ... + a_6 x^6, \tag{3}$$

$$R_{s,b} = b_0 + b_1 x + b_2 x^2 + ... + b_6 x^6, \tag{4}$$

where x is a specific SOC_b [21]. The power loss of the battery pack $P_{loss,b}$ can be written as

$$P_{loss,b} = R_{s,b} i_b^2, \tag{5}$$

where i_b is the battery current.

2) Ultracapacitor: Again for the system-level analysis, the Rint model is sufficient to represent the behavior of the UC pack [see Fig. 2]. Similarly, $V_{o,u}$ and $R_{s,c}$ are the OCV and the series resistance of the UC pack. The power loss of the UC pack $P_{loss,u}$ can be represented as

$$P_{loss,u} = R_{s,c} i_u^2, \tag{6}$$

where i_u is the UC current.

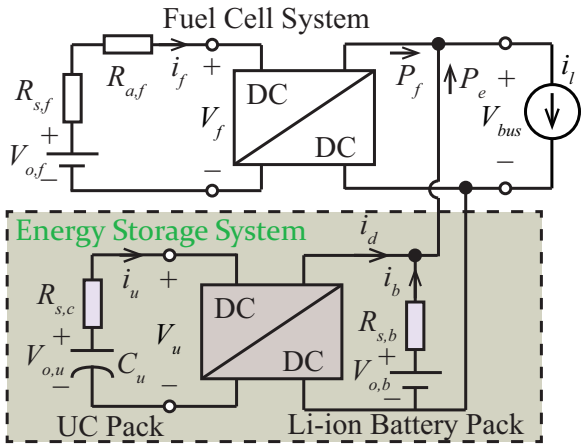

Fig. 2. Model of the fuel cell-battery-ultracapacitor hybrid system.

III. Two-Level Energy Management Strategy

In the proposed two-level energy management strategy, the battery and UC packs are seen as an ESS and ECMS is used to distribute the load power between the fuel cell system and this ESS at the first level. At the second level, the required power for the ESS is distributed between battery and UC packs using the ESR-based control strategy.

A. First level - Equivalent Consumption Minimization Strategy

For the hybrid system, the fuel cell system and ESS jointly satisfy the load demand. Intuitively, the hydrogen consumption of the fuel cell system can be reduced when the ESS supplies more power. Since ESS works as an energy buffer with zero net energy output, the ESS needs to be charged by the fuel cell system in the future to reach its initial SOC. This would lead to an extra hydrogen consumption, which may adversely affect the fuel economy. Therefore, ECMS is proposed to minimize the sum of actual hydrogen consumption from the fuel cell system and the equivalent hydrogen consumption from the ESS [16].

1) Equivalent Hydrogen Consumption: In the fuel cell based hybrid system, the total hydrogen consumption is written as

$$\dot{m}_{H_2,t} = \dot{m}_{H_2,f} + p \cdot \dot{m}_{H_2,e}, \tag{7}$$

where $\dot{m}_{H_2,e}$ is the equivalent hydrogen mass flow rate due to the usage of ESS; p is the penalty factor. Due to unknown operating conditions of the fuel cell system and the ESS, the average efficiencies of the fuel cell system and ESS are used

to convert the electrical energy into the equivalent hydrogen consumption, which can be formulated as

$$\dot{m}_{H_2,e} = \begin{cases} \dfrac{P_{e,k}}{\eta_d} \cdot \dfrac{1}{\eta_{c,a}\eta_{f,a}\mathrm{LHV}_{\mathrm{H_2}}} & \text{if } P_{e,k} > 0, \\ P_{e,k}\eta_c \cdot \dfrac{\eta_{d,a}}{\eta_{f,a}\mathrm{LHV}_{\mathrm{H_2}}} & \text{else,} \end{cases} \tag{8}$$

where $P_{e,k}$ is the power of the ESS at the time instant k; $\eta_{d,a}$ and $\eta_{c,a}$ are the average discharging and charging efficiencies of the ESS; $\eta_{f,a}$ is the average efficiency of the fuel cell system; η_d and η_c are discharging and charging efficiencies of the ESS, which are written as

$$\eta_d = \frac{P_{e,k}}{P_{e,k} + \frac{R_e P_{e,k}^2}{V_{bus,k}^2}} = \frac{1}{1 + \frac{R_e P_{e,k}}{V_{bus,k}^2}}, \tag{9}$$

$$\eta_c = \frac{P_{e,k} + \frac{R_e P_{e,k}^2}{V_{bus,k}^2}}{P_{e,k}} = 1 + \frac{R_e P_{e,k}}{V_{bus,k}^2}, \tag{10}$$

where $V_{bus,k}$ is the dc bus voltage at the time instant k; R_e is the ESR of the ESS, which is calculated from (21). Based on the power balance among the fuel cell system, the ESS, and the load, the output power of the ESS $P_{e,k}$ is expressed as

$$P_{e,k} = P_{l,k} - P_{f,k}, \tag{11}$$

where $P_{f,k}$ and $P_{l,k}$ are the fuel cell power and the load power at the time instant k, respectively. Then, substituting (1), (8)–(11) into (7), $\dot{m}_{H_2,t}$ can be rewritten as

$$\dot{m}_{H_2,t} = \left(a_{f_0} + p\frac{R_e K_1}{V_{bus,k}^2}\right) P_{f,k}^2 - \left[pK_1\left(\frac{2R_e}{V_{bus,k}^2}P_{l,k} + 1\right) - a_{f_1}\right] P_{f,k} + a_{f_2} + pK_1 P_{l,k}\left(1 + \frac{R_e}{V_{bus,k}^2}P_{l,k}\right), \tag{12}$$

$$K_1 = \begin{cases} K_{1^+} = \dfrac{1}{\eta_{c,a}\eta_{f,a}\mathrm{LHV}_{H_2}} & P_{e,k} > 0, \\ K_{1^-} = \dfrac{\eta_{d,a}}{\eta_{f,a}\mathrm{LHV}_{H_2}} & P_{e,k} < 0. \end{cases} \tag{13}$$

Because $\dot{m}_{H_2,t}$ is a quadratic function of P_f and $\left(a_{f_0} + p\frac{R_e K_1}{V_{bus,k}^2}\right)$ is positive, the output power of the fuel cell system $P_{f,k}$ at the time instant k can be analytically derived, as shown in (14). In (14), $P_{f,max}$ is the maximum power of the fuel cell system. For the obtained two points $P_{f1,k}$ and $P_{f2,k}$, the one with the lower hydrogen consumption is used as the output power of the fuel cell system.

2) Penalty Factor: In the ECMS, the output power of the fuel cell system is related to the penalty factor p, which needs to be tuned to maintain the SOC of the ESS SOC_e around its initial value $\mathrm{SOC}_{e,i}$. Due to the limited energy density of UCs, the SOC of the ESS refers to the SOC of the battery pack [18]. In this paper, the penalty factor p is formulated as

$$p = \left[p_m + (p_h - p_m)\frac{\mathrm{SOC}_e - \mathrm{SOC}_{e,i}}{\mathrm{SOC}_{e,h} - \mathrm{SOC}_{e,i}}\right]^{\frac{1+s_1}{2}} \cdot \left[p_m + (p_l - p_m)\frac{\mathrm{SOC}_e - \mathrm{SOC}_{e,i}}{\mathrm{SOC}_{e,l} - \mathrm{SOC}_{e,i}}\right]^{\frac{1-s_1}{2}}, \tag{15}$$

$$s_1 = \mathrm{sign}(\mathrm{SOC}_e - \mathrm{SOC}_{e,i})$$

$$p_h = \frac{a_{f_1}}{K_1(\frac{2R_e}{V_{bus,k}^2}P_{l,k} + 1)}, \quad p_l = \frac{2a_{f_0}P_{f,max} + a_{f_1}}{K_1\left[\frac{2R_e}{V_{bus,k}^2}(P_{l,k} - P_{f,max}) + 1\right]},$$

$$p_m = \frac{2a_{f_0}P_{l,a} + a_{f_1}}{K_1\left[\frac{2R_e}{V_{bus,k}^2}(P_{l,k} - P_{l,a}) + 1\right]}, \tag{16}$$

where $\mathrm{SOC}_{e,h}$ and $\mathrm{SOC}_{e,l}$ are upper and lower limits of the SOC of the ESS. The relationship between the output power

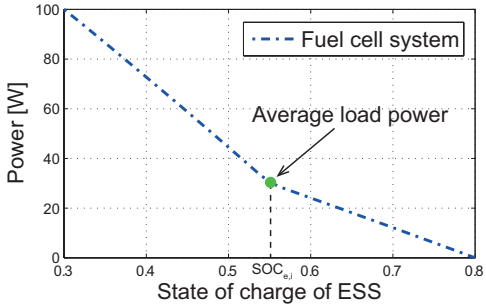

Fig. 3. Output power of the fuel cell system.

of the fuel cell system and the SOC_e is shown in Fig. 3. It shows that P_f is equal to the average load power $P_{l,a}$ when SOC_e is equal to $\mathrm{SOC}_{e,i}$, as shown in Fig. 3. If SOC_e is smaller than $\mathrm{SOC}_{e,i}$, P_f becomes larger than $P_{l,a}$ to charge the ESS. For the extreme case with a minimum SOC_e, the fuel cell system supplies its maximum power $P_{f,max}$ to supply the load demand. Similarly, when SOC_e is higher than $\mathrm{SOC}_{e,i}$, the output power of the fuel cell system P_f becomes smaller than $P_{l,a}$ and the rest power is drawn from the ESS. Due to the slow dynamics of the fuel cell system, a first-order low-pass filter with a time constant τ_f is used to smoothen the output power of the fuel cell system and avoid fuel cell starvation [22]. Without a prior knowledge of the load profile

$$P_{f,k} = \begin{cases} P_{f1,k} = \mathrm{Min}\left[\mathrm{Max}\left(\dfrac{pK_{1^+}\left(\frac{2R_e}{V_{bus,k}^2}P_{l,k} + 1\right) - a_{f_1}}{2a_{f_0} + pK_{1^+}\frac{2R_e}{V_{bus,k}^2}}, 0\right), P_{l,k}\right] & P_{e,k} > 0, \\ P_{f2,k} = \mathrm{Min}\left[\mathrm{Max}\left(\dfrac{pK_{1^-}\left(\frac{2R_e}{V_{bus,k}^2}P_{l,k} + 1\right) - a_{f_1}}{2a_{f_0} + pK_{1^-}\frac{2R_e}{V_{bus,k}^2}}, P_{l,k}\right), P_{f,max}\right] & P_{e,k} \le 0, \end{cases} \tag{14}$$

in real applications, a moving average filter is used to estimate the average load power based on the past N_1 seconds, which is calculated as

$$P_{l,a,k}^{N_1} = \begin{cases} \frac{1}{k}\left(P_{l,a,k-1}^{N_1} \cdot (k-1) + P_{l,k}\right) & \text{if } k \le N_1, \\ \frac{1}{N_1}\left(P_{l,a,k-1}^{N_1} \cdot N + P_{l,k} - P_{l,k-N_1}\right) & \text{else.} \end{cases}$$

Then, $P_{l,a,k}^{N_1}$ is used to calculate p_m in (16) for real-time implementation.

B. Second level - Equivalent Series Resistance-based Control

In this level, the power distribution between battery and UC packs is determined using the ESR-based approach [23]. In the ESR-based control strategy, the estimated average load current is supplied by the battery pack and the remaining dynamic load current is distributed between battery and UC packs based on their ESR ratio.

1) Equivalent Series Resistance Ratio: In the battery-UC hybrid system, a half-bridge bidirectional dc-dc converter is placed between UC pack and the load and the battery pack is directly connected to the load, as shown in Fig. 2. Since the switching frequency of the dc-dc converter is constant, its switching loss is almost constant and irrelevant to the operating conditions. Thus, only the conduction losses of the MOSFET and the inductor in the dc-dc converter are considered. Therefore, the ESRs of each component are calculated as

$$K_2 = \frac{R_b^*}{R_d^* + R_u^*}, \quad R_d^* = \frac{P_{loss,d}}{i_d^2} = \frac{R_L + R_{mos}}{(1-d_s)^2},$$
$$R_b^* = \frac{P_{loss,b}}{i_d^2} = R_{s,b}, \quad R_u^* = \frac{P_{loss,u}}{i_u^2} = \frac{R_{s,c}}{(1-d_s)^2},$$

where d_s is the duty cycle of the dc-dc converter; R_L and R_{mos} are resistances of the inductor and the MOSFET, respectively; K_2 is the ESR ratio between battery and UC packs.

2) Current Distribution: In the ESR-based strategy, the dynamic load current for the battery-UC hybrid system is distributed based on the ESR ratio and the SOC of the UC pack. The current distribution is expressed as

$$C_d = Q\frac{1}{1+K_2}, \tag{17}$$

where Q is the UC energy sustaining factor, which is designed to force SOC_u to swing around its initial value $\mathrm{SOC}_{u,i}$. Therefore, Q is written as

$$Q = \begin{cases} \frac{\mathrm{SOC}_u - \mathrm{SOC}_{u,i}}{\mathrm{SOC}_{u,i} - \mathrm{SOC}_{u,l}} K_{2^-}^{\frac{1+s_2}{2}} + 1 & \text{if } i_{e,d,k} \le 0, \\ \frac{\mathrm{SOC}_u - \mathrm{SOC}_{u,i}}{\mathrm{SOC}_{u,i} - \mathrm{SOC}_{u,h}} K_{2^+}^{\frac{1-s_2}{2}} + 1 & \text{else,} \end{cases} \tag{18}$$

$$K_{2^-} = \frac{\mathrm{SOC}_{u,i} - \mathrm{SOC}_{u,l}}{\mathrm{SOC}_{u,h} - \mathrm{SOC}_{u,i}} K_2, K_{2^+} = \frac{\mathrm{SOC}_{u,i} - \mathrm{SOC}_{u,h}}{\mathrm{SOC}_{u,l} - \mathrm{SOC}_{u,i}} K_2,$$
$$s_2 = \mathrm{sign}(\mathrm{SOC}_u - \mathrm{SOC}_{u,i}), \quad \mathrm{SOC}_u = \frac{V_{u,k}^2 - V_{u,min}^2}{V_{u,max}^2 - V_{u,min}^2},$$

where $V_{u,k}$ is the voltage of the UC pack at the time instant k; $V_{u,min}$ and $V_{u,max}$ are the minimum and maximum voltages of the UC pack; $\mathrm{SOC}_{u,h}$ and $\mathrm{SOC}_{u,l}$ are upper and lower limits of SOC_u. Similarly, the moving average filter with window size N_2 is used to estimate the average current of the ESS $I_{e,a,k}^{N_2}$ in real applications. Then, the currents of the battery pack $i_{b,k}$ and the dc-dc converter $i_{d,k}$ are written as

$$i_{b,k} = I_{e,a,k}^{N_2} + C_d(i_{e,k} - I_{e,a,k}^{N_2}), \quad i_{d,k} = i_{e,k} - i_{b,k}. \tag{19}$$

where $i_{e,k}$ is the current of the ESS and is $\frac{P_{e,k}}{V_{bus,k}}$. The power loss of the ESS $P_{loss,e,k}$ is calculated as

$$\begin{aligned} P_{loss,e,k} =& i_{b,k}^2 R_b^* + i_{d,k}^2 (R_d^* + R_u^*), \\ =& \left[I_{e,a,k}^{N_2} + C_d(i_{e,k} - I_{e,a,k}^{N_2})\right]^2 R_b^* \\ &+ (1-C_d)^2 (i_{e,k} - I_{e,a,k}^{N_2})^2 (R_d^* + R_u^*), \end{aligned} \tag{20}$$

and the ESR of the ESS R_e is expressed as

$$\begin{aligned} R_e =& \frac{P_{loss,e,k}}{i_{e,k}^2} = \left[C_d + (1-C_d^*)\frac{I_{e,a,k}^{N_2}}{i_{e,k}}\right]^2 R_b^* \\ &+ (1-C_d)^2 \left(1 - \frac{I_{l,a,k}^{N_2}}{i_{e,k}}\right)^2 (R_d^* + R_u^*). \end{aligned} \tag{21}$$

Then in the proposed energy management strategy, R_e calculated at the time instant $k-1$ is used to calculate the output power of the fuel cell system $P_{f,k}$ in (14) and penalty factor p in (15). The block diagram of the two-level energy management strategy is shown in Fig. 4. Based on the estimated average load power $P_{l,a,k}^{N_1}$, the penalty factor is calculated using (15). Then the fuel cell power $P_{f,k}$ is calculated from (14). To avoid fuel cell starvation problem, its reference output power $P_{f,ref,k}$ is obtained by using a first-order low-pass filter [18]. Thus, the current of the ESS $i_{e,k}$ is calculated and distributed between battery and UC packs based on the current distribution C_d and estimated average current $I_{e,a,k}^{N_2}$.

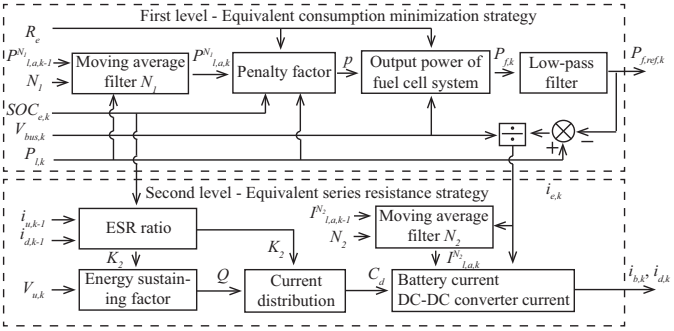

Fig. 4. Block diagram of the two-level energy management strategy.

IV. Simulation and Discussions

In simulation, three consecutive repetitions of the scaled new European driving cycle (NEDC) test cycle is used as the load profile. Fig. 5 shows the downscaled power profile of the NEDC, which is calculated based on the vehicle dynamics

TABLE I
PARAMETERS FOR FUEL CELL-BATTERY-ULTRACAPACITOR HYBRID SYSTEM.

Fuel cell system										
$a_{f,0}$	6.7033e^{-8}	$a_{f,1}$	1.2487e^{-5}	$a_{f,2}$	4.0458e^{-5}	τ_f	7 s	$\eta_{f,a}$	0.45	
Battery pack										
a_0	12.38	a_1	29.02	a_2	-129.51	a_3	299.09	a_4	-366.81	a_5	231.77
a_6	-59.23	b_0	0.49	b_1	-4.72	b_2	28.51	b_3	-83.27	b_4	125.62
b_5	-94.10	b_6	27.67							
UC pack				DC-DC converter				Energy storage system			
C_u	66 F	$R_{s,c}$	15 mΩ	R_{mos}	15 mΩ	R_L	10 mΩ	$\eta_{c,a}$	0.93	$\eta_{d,a}$	0.93

and scaled down to match the power capability of the proposed hybrid system. The model parameters are listed in Table I. For the ESS, $\mathrm{SOC}_{e,h}$, $\mathrm{SOC}_{e,i}$, and $\mathrm{SOC}_{e,l}$ are set to be 0.80, 0.55, and 0.30, respectively. For the UC pack, $\mathrm{SOC}_{u,h}$, $\mathrm{SOC}_{u,i}$, and $\mathrm{SOC}_{u,l}$ are set to be 1.0, 0.5, and 0, respectively. The total hydrogen consumption over the load profile $m_{H_2,t}$ is calculated as

$$\begin{aligned} m_{H_2,t} &= \sum_{k=1}^{N} \dot{m}_{H_2,f,k} T_s + m_{H_2,e}, \\ \Delta E_e &= \sum_{k=1}^{N} \left(V_{o,b,k} i_{b,k} + V_{o,u,k} i_{u,k} \right) T_s, \\ m_{H_2,e} &= \begin{cases} \dfrac{\Delta E_e}{\eta_{d,a}\eta_{c,a}\eta_{f,a}\mathrm{LHV}_{\mathrm{H_2}}} & \text{if } \Delta E_e > 0, \\ \dfrac{\Delta E_e \eta_{c,a}\eta_{d,a}}{\eta_{f,a}\mathrm{LHV}_{\mathrm{H_2}}} & \text{else,} \end{cases} \end{aligned} \tag{22}$$

where ΔE_e is the net energy output of the ESS; $m_{H_2,f,k}$ is the hydrogen mass flow rate of the fuel cell system at the time instant k; $m_{H_2,e}$ is the equivalent hydrogen consumption due to ΔE_e.

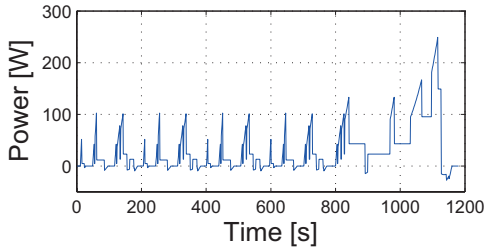

Fig. 5. Downscaled power profile of the NEDC.

A. Influence of Window Size

The total hydrogen consumptions of the fuel cell-battery-UC hybrid system using the proposed two-level energy management strategy are shown in Fig. 6. Due to the relative low efficiency of the fuel cell system, the influence of N_1 is larger than that of N_2. Note that the nonlinear relationship exists between $m_{H_2,t}$ and the window size. This means accurate estimated average values of $P_{l,a}$ and $I_{e,a}$ with large window sizes does not guarantee low hydrogen consumption. At the same time, the optimal window sizes N_1 and N_2 are 1400 s and 1200 s, respectively, which are close to the length of the NEDC test cycle. It indicates design of the window size based on the length of the typical load profile can effectively reduce the fuel consumption.

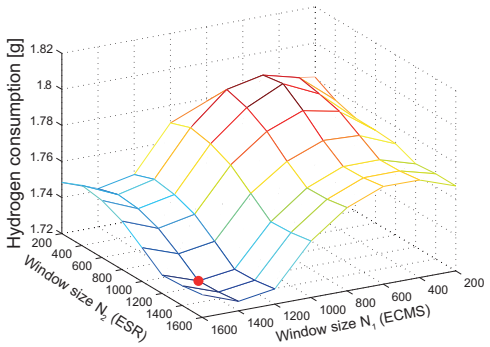

Fig. 6. Total hydrogen consumption as a function of window sizes N_1 and N_2.

B. Comparison with Rule-based Strategy

For comparison purposes, the performance of the proposed two-level energy management strategy is compared with the rule-based strategy. In the rule-based strategy, the output power of the fuel cell system is determined based on the SOC of the battery pack and the load power, as shown in Table II [24]. Similarly, a first-order low-pass filter is used to restrict the power slope of the fuel cell system. The power distribution between battery and UC packs is determined based on the SOC of the UC pack using a look-up table [25].

TABLE II
RULE-BASED CONTROL STRATEGY.

If $\mathrm{SOC}_e < 0.53$	P_f=$P_{f,max}$
If $\mathrm{SOC}_e \subset (0.53, 0.60)$ and $P_l > 160$	P_f=$P_{f,max}$
If $\mathrm{SOC}_e \subset (0.53, 0.60)$ and $P_l < 160$	P_f=$P_{f,opt}$
If $\mathrm{SOC}_e > 0.60$	P_f=0

TABLE III
RESULTS OF THE PROPOSED TWO-LEVEL AND RULE-BASED STRATEGIES.

Control strategy	m_{H_2}[g]	$\Delta\mathrm{SOC}_b$	$\Delta\mathrm{SOC}_u$
Two-level	1.723	0.060	0.878
Rule-based	1.782	0.048	0.908

The performance of the proposed two-level energy management strategy is compared with the rule-based strategy under

three consecutive repetitions of the scaled NEDC test cycle, as shown in Fig. 7 and Table III. In Table III, $\Delta\mathrm{SOC}_b$ and $\Delta\mathrm{SOC}_u$ denote the SOC variation ranges of the battery and UC packs, respectively. For a fair comparison, the parameters of the rule-based strategy are tuned to make sure $\Delta\mathrm{SOC}_b$ using two control strategies are close. Results show that the proposed two-level strategy can achieve lower hydrogen consumption compared with the rule-based strategy. This is because the fuel cell system operates at its maximum power point (low-efficiency working point) with a low SOC_e in the rule-based strategy, which leads to extra hydrogen consumption, as shown in Fig. 7. Fig. 7(a) indicates that through considering the hydrogen consumption model of the fuel cell system, the proposed two-level energy management strategy can maintain the fuel cell system operate at its efficient region.

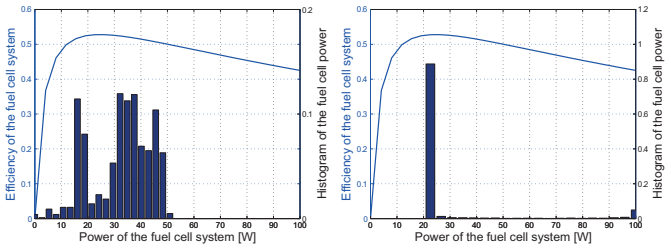

(a) (b)

Fig. 7. Histogram of the fuel cell power. (a) Rule-based strategy. (b) Two-level strategy.

V. Conclusion

In this paper a two-level energy management strategy is proposed for the fuel cell-battery-UC hybrid system. At the first level, battery and UC packs are treated as an ESS and the load power is distributed between the fuel cell system and this ESS using the ECMS. The penalty factor is tuned based on the SOC of the battery pack and the estimated average load power over past N_1 seconds. At the second level, the load demand for the ESS is distributed between the battery and UC packs using the ESR-based control strategy. In the ESR-based strategy, the average current during the past N_2 is supplied by the battery pack and the remaining dynamic load power is distributed between battery and UC packs based on their ESR ratio. Simulation results show that the optimal window sizes N_1 and N_2 are close to the length of the typical load profile. Compared with the rule-based strategy, the proposed two-level energy management strategy can achieve lower hydrogen consumption.

References

[1] T. Matsumoto, N. Watanabe, H. Sugiura, and T. Ishikawa, "Development of fuel-cell hybrid vehicle," *SAE TRANSACTIONS*, vol. 111, no. 3, pp. 376–382, 2002.

[2] W. Schmittinger and A. Vahidi, "A review of the main parameters influencing long-term performance and durability of pem fuel cells," *J. Power Sources*, vol. 180, no. 1, pp. 1–14, 2008.

[3] J. Bernard, S. Delprat, F. N. Büchi, and T. M. Guerra, "Fuel-cell hybrid powertrain: Toward minimization of hydrogen consumption," *IEEE Trans. Veh. Technol.*, vol. 58, no. 7, pp. 3168–3176, 2009.

[4] W. Gao, "Performance comparison of a fuel cell-battery hybrid powertrain and a fuel cell-ultracapacitor hybrid powertrain," *IEEE Trans. Veh. Technol.*, vol. 54, no. 3, pp. 846–855, 2005.

[5] B. Vural, S. Dusmez, M. Uzunoglu, E. Ugur, and B. Akin, "Fuel consumption comparison of different battery/ultracapacitor hybridization topologies for fuel-cell vehicles on a test bench," *IEEE J. Emerging Sel. Topics Power Electron.*, vol. 2, no. 3, pp. 552–561, 2014.

[6] J. Bauman and M. Kazerani, "A comparative study of fuel-cell–battery, fuel-cell–ultracapacitor, and fuel-cell–battery–ultracapacitor vehicles," *IEEE Trans. Veh. Technol.*, vol. 57, no. 2, pp. 760–769, 2008.

[7] Z. Jiang and R. A. Dougal, "A compact digitally controlled fuel cell/battery hybrid power source," *IEEE Trans. Ind. Electron.*, vol. 53, no. 4, pp. 1094–1104, 2006.

[8] M. Ortúzar, J. Moreno, and J. Dixon, "Ultracapacitor-based auxiliary energy system for an electric vehicle: Implementation and evaluation," *IEEE Trans. Ind. Electron.*, vol. 54, no. 4, pp. 2147–2156, 2007.

[9] P. Thounthong, V. Chunkag, P. Sethakul, B. Davat, and M. Hinaje, "Comparative study of fuel-cell vehicle hybridization with battery or supercapacitor storage device," *IEEE Trans. Veh. Technol.*, vol. 58, no. 8, pp. 3892–3904, 2009.

[10] M. Zandi, A. Payman, J.-P. Martin, S. Pierfederici, B. Davat, and F. Meibody-Tabar, "Energy management of a fuel cell/supercapacitor/battery power source for electric vehicular applications," *IEEE Trans. Veh. Technol.*, vol. 60, pp. 433–443, Feb. 2011.

[11] M. Hannan, F. Azidin, and A. Mohamed, "Multi-sources model and control algorithm of an energy management system for light electric vehicles," *Energy Convers. Manage.*, vol. 62, pp. 123–130, 2012.

[12] S. Zhang and R. Xiong, "Adaptive energy management of a plug-in hybrid electric vehicle based on driving pattern recognition and dynamic programming," *Appl. Energy*, vol. 155, pp. 68–78, 2015.

[13] R. T. Bambang, A. S. Rohman, C. J. Dronkers, R. Ortega, A. Sasongko *et al.*, "Energy management of fuel cell/battery/supercapacitor hybrid power sources using model predictive control," *IEEE Trans. Ind. Inf.*, vol. 10, no. 4, pp. 1992–2002, 2014.

[14] J. P. Torreglosa, P. Garcia, L. M. Fernandez, and F. Jurado, "Predictive control for the energy management of a fuel-cell–battery–supercapacitor tramway," *IEEE Trans. Ind. Inf.*, vol. 10, no. 1, pp. 276–285, 2014.

[15] Q. Li, W. Chen, Z. Liu, M. Li, and L. Ma, "Development of energy management system based on a power sharing strategy for a fuel cell-battery-supercapacitor hybrid tramway," *J. Power Sources*, vol. 279, pp. 267–280, 2015.

[16] P. Rodatz, G. Paganelli, A. Sciarretta, and L. Guzzella, "Optimal power management of an experimental fuel cell/supercapacitor-powered hybrid vehicle," *Control Engineering Practice*, vol. 13, no. 1, pp. 41–53, 2005.

[17] N. Kim, S. Cha, and H. Peng, "Optimal control of hybrid electric vehicles based on pontryagin's minimum principle," *IEEE Trans. Control Systems Technology*, vol. 19, no. 5, pp. 1279–1287, 2011.

[18] P. García, J. P. Torreglosa, L. M. Fernández, and F. Jurado, "Viability study of a FC-battery-SC tramway controlled by equivalent consumption minimization strategy," *Int. J. Hydrogen Energy*, vol. 37, no. 11, pp. 9368–9382, 2012.

[19] S. Haji, "Analytical modeling of pem fuel cell i-V curve," *Renewable Energy*, vol. 36, no. 2, pp. 451–458, 2011.

[20] E. Tazelaar, B. Veenhuizen, P. van den Bosch, and M. Grimminck, "Analytical solution of the energy management for fuel cell hybrid propulsion systems," *IEEE Trans. Veh. Technol.*, vol. 61, no. 5, pp. 1986–1998, 2012.

[21] R. C. Kroeze and P. T. Krein, "Electrical battery model for use in dynamic electric vehicle simulations," in *Proc. IEEE Power Electronics Specialists (PESC'2008)*, Rhodes, Greece, Jun. 2008, pp. 1336–1342.

[22] A. Payman, S. Pierfederici, and F. Meibody-Tabar, "Energy management in a fuel cell/supercapacitor multisource/multiload electrical hybrid system," *IEEE Trans. Power Electron.*, vol. 24, no. 12, pp. 2681–2691, 2009.

[23] C. Zhao, H. Yin, Z. Yang, and C. Ma, "Equivalent series resistance-based real-time control for a battery-ultracapacitor hybrid system," in *Proc. IECON 2015*. IEEE, 2015, pp. 001 849–001 854.

[24] P. Garcia, L. M. Fernandez, C. A. Garcia, and F. Jurado, "Energy management system of fuel-cell-battery hybrid tramway," *IEEE Trans. Ind. Electron.*, vol. 57, no. 12, pp. 4013–4023, 2010.

[25] J. Shen, S. Dusmez, and A. Khaligh, "Optimization of sizing and battery cycle life in battery/UC hybrid energy storage system for electric vehicle applications," *IEEE Trans. Ind. Inf.*, vol. 10, no. 4, pp. 2112–2121, 2014.